

Chfr is required for tumor suppression and Aurora A regulation

Xiaochun Yu¹, Katherine Minter-Dykhouse¹, Liviu Malureanu², Wei-Meng Zhao³, Dongwei Zhang⁴, Carolin J Merkle¹, Irene M Ward¹, Hideyuki Saya⁴, Guowei Fang³, Jan van Deursen² & Junjie Chen¹

Tumorigenesis is a consequence of loss of tumor suppressors and activation of oncogenes. Expression of the mitotic checkpoint protein Chfr is lost in 20–50% of primary tumors and tumor cell lines. To explore whether downregulation of Chfr contributes directly to tumorigenesis, we generated Chfr knockout mice. Chfr-deficient mice are cancer-prone, develop spontaneous tumors and have increased skin tumor incidence after treatment with dimethylbenz(a)anthracene. Chfr deficiency leads to chromosomal instability in embryonic fibroblasts and regulates the mitotic kinase Aurora A, which is frequently upregulated in a variety of tumors. Chfr physically interacts with Aurora A and ubiquitinates Aurora A both *in vitro* and *in vivo*. Collectively, our data suggest that Chfr is a tumor suppressor and ensures chromosomal stability by controlling the expression levels of key mitotic proteins such as Aurora A.

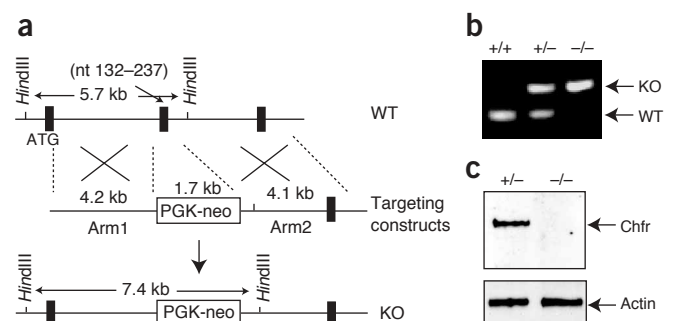
Precise regulation of DNA condensation and chromosome segregation in mitosis is important for normal cell cycle progression. The progression of cells in mitosis is driven by several key mitotic kinases including CDC2, PLK1 and Aurora kinases. Failure or improper regulation of these kinases leads to aneuploidy and may contribute to tumorigenesis in humans. For example, Aurora A kinase is overexpressed or amplified in a number of primary tumors and tumor cell lines^{1,2}. Mouse NIH-3T3 cells transfected with Aurora A develop into tumors when implanted in nude mice, suggesting that Aurora A is oncogenic^{3–5}.

The most studied mitotic checkpoint is the spindle assembly checkpoint. Proteins involved in the spindle checkpoint sense microtubule-

kinetochore attachment and allow the activation of the anaphase-promoting complex (APC) only when all chromosomes are properly attached to the spindles and aligned on the metaphase plate^{6–8}. Although the integrity of the spindle checkpoint is essential for the maintenance of chromosomal stability, spindle checkpoint proteins and APC components are rarely downregulated or mutated in tumors^{9,10}, suggesting that the disruption of other mitotic checkpoint pathways may have a greater role in tumor-associated chromosomal instability.

Chfr (checkpoint protein with FHA and Ring domain) was recently identified as defining a new early mitotic checkpoint that delays transition to metaphase in response to mitotic stress^{11,12}. The physiological function of Chfr is still not known. Chfr contains an N-terminal FHA domain¹³, which is involved in phosphoprotein interaction, and a Ring domain, which participates in protein ubiquitination. The putative Chfr fission yeast ortholog Dma1 also contains both an FHA domain and a Ring domain and participates in multiple mitotic events, including CDC2 activation, spindle assembly and cytokinesis^{14,15}. The Ring domain of Chfr has E3 ubiquitin ligase activity *in vitro*^{16–18}. One potential Chfr substrate is PLK1 (ref. 16), but the expression of PLK1 does not always correlate with Chfr downregulation and Chfr function in breast cancer cell lines, suggesting that other Chfr substrates are involved in mitotic checkpoint control¹⁹. Although Chfr is ubiquitously expressed in normal tissues, it is frequently downregulated in human cancers, mostly owing to hypermethylation of its promoter region^{20–25}. Chfr downregulation

Figure 1 Targeted disruption of *Chfr* in mice. (a) Strategy for generating the targeted *Chfr* allele. Part of mouse *Chfr* (WT; top), the targeting vector (middle) and the disrupted *Chfr* allele (KO; bottom) are shown. (b) Multiplex PCR genotype analyses for *neo* (KO; upper band) and the targeted exon (WT; lower band) were done to confirm the genotypes of wild-type and Chfr-deficient mice. (c) Western blots of cell lysates prepared from MEFs with indicated genotypes were done with immunoprecipitates using antibody to Chfr (upper panel). Immunoblotting with antibody to actin was used as loading control (lower panel).



¹Department of Oncology, and ²Pediatric and Adolescent Medicine, Mayo Clinic and Foundation, Rochester, Minnesota 55905, USA. ³Department of Biological Sciences, Stanford University, Stanford, California 94305, USA. ⁴Department of Tumor Genetics and Biology, Kumamoto University, Kumamoto, 860-8556, Japan. Correspondence should be addressed to J.C. (chen.junjie@mayo.edu).

Published online 27 March 2005; doi:10.1038/ng1538

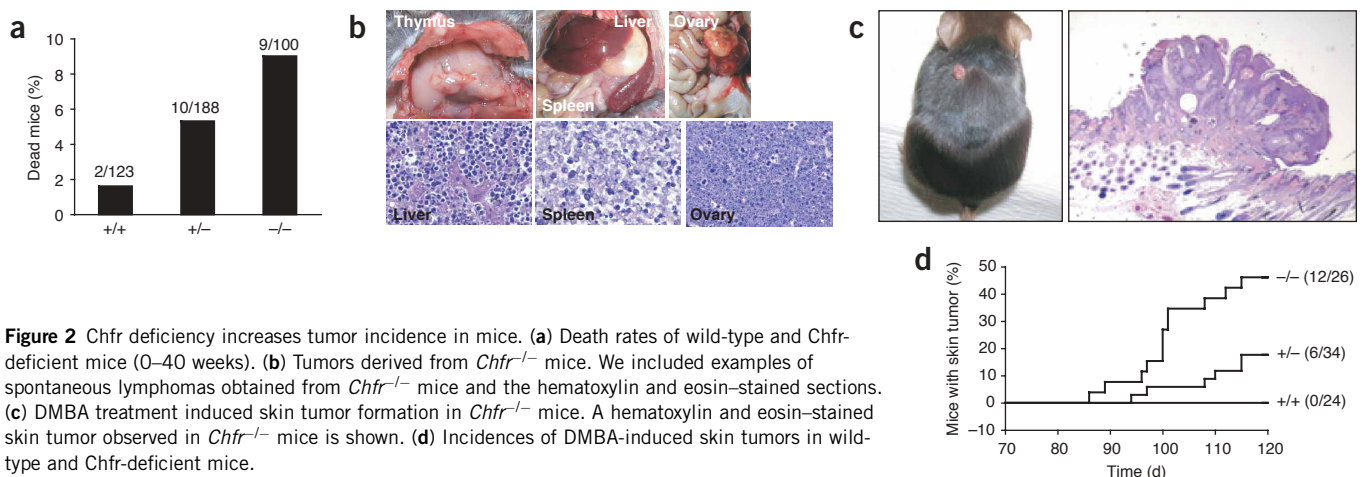


Figure 2 *Chfr* deficiency increases tumor incidence in mice. **(a)** Death rates of wild-type and *Chfr*-deficient mice (0–40 weeks). **(b)** Tumors derived from *Chfr*^{-/-} mice. We included examples of spontaneous lymphomas obtained from *Chfr*^{-/-} mice and the hematoxylin and eosin–stained sections. **(c)** DMBA treatment induced skin tumor formation in *Chfr*^{-/-} mice. A hematoxylin and eosin–stained skin tumor observed in *Chfr*^{-/-} mice is shown. **(d)** Incidences of DMBA-induced skin tumors in wild-type and *Chfr*-deficient mice.

has been found in primary lung, colon, esophagus and gastric carcinomas and tumor cell lines of lung, colon, esophageal, brain, bone, breast, gastric and hematopoietic origin^{11,19–25}. Mutations in *CHFR* have also been identified in primary lung cancers and cell lines including osteosarcoma and breast cancer^{11,19,24}. These observations raise the possibility that *Chfr* may contribute to tumorigenesis in humans.

To explore the physiological function of *Chfr* and its role in tumorigenesis, we generated *Chfr*-null mice by disrupting *Chfr* using standard gene-targeting techniques. We replaced an exon that encodes part of the sequence of the *Chfr* FHA domain with a neomycin

selection cassette (**Fig. 1a**). We used two independent embryonic stem (ES) cell clones to generate *Chfr*-deficient mice. We carried out PCR analyses to confirm that we obtained mice of genotype *Chfr*^{-/-} (**Fig. 1b**). We also confirmed by western blotting using antibodies to *Chfr* that *Chfr* was not expressed in *Chfr*^{-/-} mice (**Fig. 1c**).

Chfr^{-/-} mice were viable and had no obvious developmental defects, suggesting that *Chfr* is not required for normal cell cycle progression during embryonic development. We proceeded to monitor tumor incidence in these mice over time. After 40 weeks, nine *Chfr*^{-/-} mice (9%) developed lymphoma, which invaded thymus, spleen, liver and ovary (**Fig. 2a,b**), and died. Ten *Chfr*^{+/-} mice (5.3%)

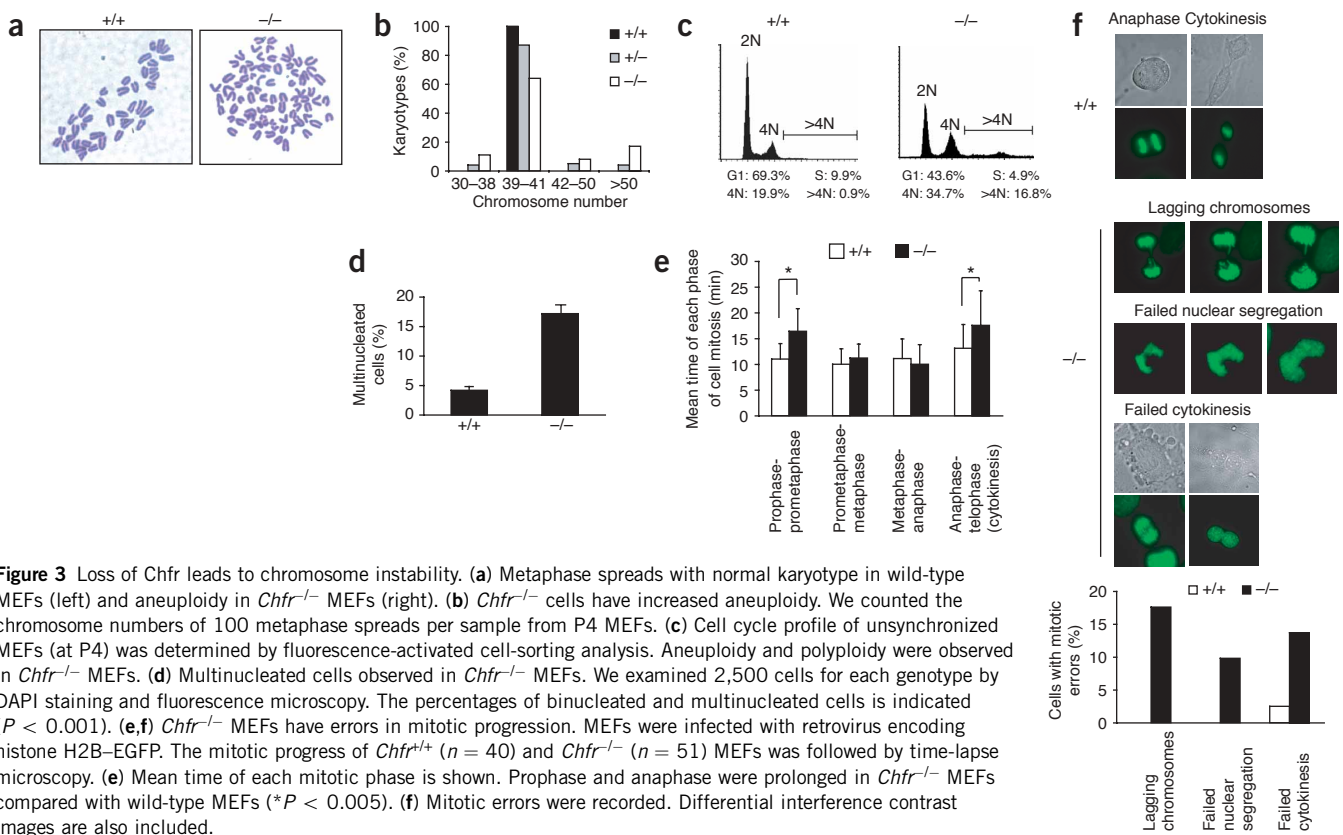


Figure 3 Loss of *Chfr* leads to chromosome instability. **(a)** Metaphase spreads with normal karyotype in wild-type MEFs (left) and aneuploidy in *Chfr*^{-/-} MEFs (right). **(b)** *Chfr*^{-/-} cells have increased aneuploidy. We counted the chromosome numbers of 100 metaphase spreads per sample from P4 MEFs. **(c)** Cell cycle profile of unsynchronized MEFs (at P4) was determined by fluorescence-activated cell-sorting analysis. Aneuploidy and polyploidy were observed in *Chfr*^{-/-} MEFs. **(d)** Multinucleated cells observed in *Chfr*^{-/-} MEFs. We examined 2,500 cells for each genotype by DAPI staining and fluorescence microscopy. The percentages of binucleated and multinucleated cells is indicated ($P < 0.001$). **(e,f)** *Chfr*^{-/-} MEFs have errors in mitotic progression. MEFs were infected with retrovirus encoding histone H2B–EGFP. The mitotic progress of *Chfr*^{+/+} ($n = 40$) and *Chfr*^{-/-} ($n = 51$) MEFs was followed by time-lapse microscopy. **(e)** Mean time of each mitotic phase is shown. Prophase and anaphase were prolonged in *Chfr*^{-/-} MEFs compared with wild-type MEFs ($*P < 0.005$). **(f)** Mitotic errors were recorded. Differential interference contrast images are also included.

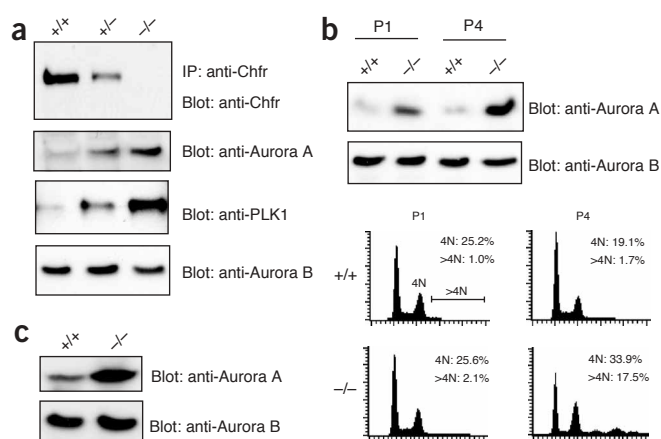


Figure 4 Chfr negatively regulates expression of Aurora A. (a) Expression of Aurora A was upregulated in *Chfr*^{-/-} MEFs. Lysates derived from wild-type or *Chfr*-deficient MEFs were immunoprecipitated (IP) and immunoblotted with indicated antibodies. (b) Aurora A levels were determined using P1 or P4 wild-type and *Chfr*^{-/-} MEFs. Cell lysates were blotted with the indicated antibodies. Cell cycle distributions were determined by fluorescence-activated cell-sorting analysis. (c) Expression of Aurora A was higher in *Chfr*^{-/-} tissues. Liver and spleen were homogenized and lysed. Lysates were immunoblotted with indicated antibodies.

also died during this period from lymphoma (Fig. 2a and data not shown). Only two wild-type mice (1.6%) died during this period, and we observed no tumors in wild-type mice. From 40 to 80 weeks, 38 *Chfr*^{-/-} mice died. At least 29 of them had obvious tumors in gross pathological examination. Most tumors found during this period were epithelial tumors in major organs, especially lung, liver and gastrointestinal tract (Supplementary Fig. 1 and Supplementary Table 1

online). In the same time frame, eight *Chfr*^{+/+} mice died, three of which had tumors. Tumor incidence in *Chfr*^{+/+} mice was intermediate between that in *Chfr*^{+/+} and *Chfr*^{-/-} mice. The spectrum of tumors identified in *Chfr*^{+/+} mice was similar to that in *Chfr*^{-/-} mice. The higher death rate and tumor incidence in *Chfr*^{-/-} mice suggest that Chfr is important for tumor suppression. To confirm that Chfr deficiency leads to increased tumor incidence, we treated wild-type and *Chfr*-deficient mice with a single dose of dimethylbenz(a)anthracene (DMBA), a chemical carcinogen, on the dorsal skin 3–5 d after birth. After 4 months, nearly 50% of *Chfr*^{-/-} mice, but no wild-type mice, developed skin tumors (Fig. 2c,d). *Chfr*^{+/+} mice also developed skin tumors, albeit at a lower frequency than *Chfr*^{-/-} mice (Fig. 2d). Taken together, these results support the idea that Chfr is required for tumor suppression in mice.

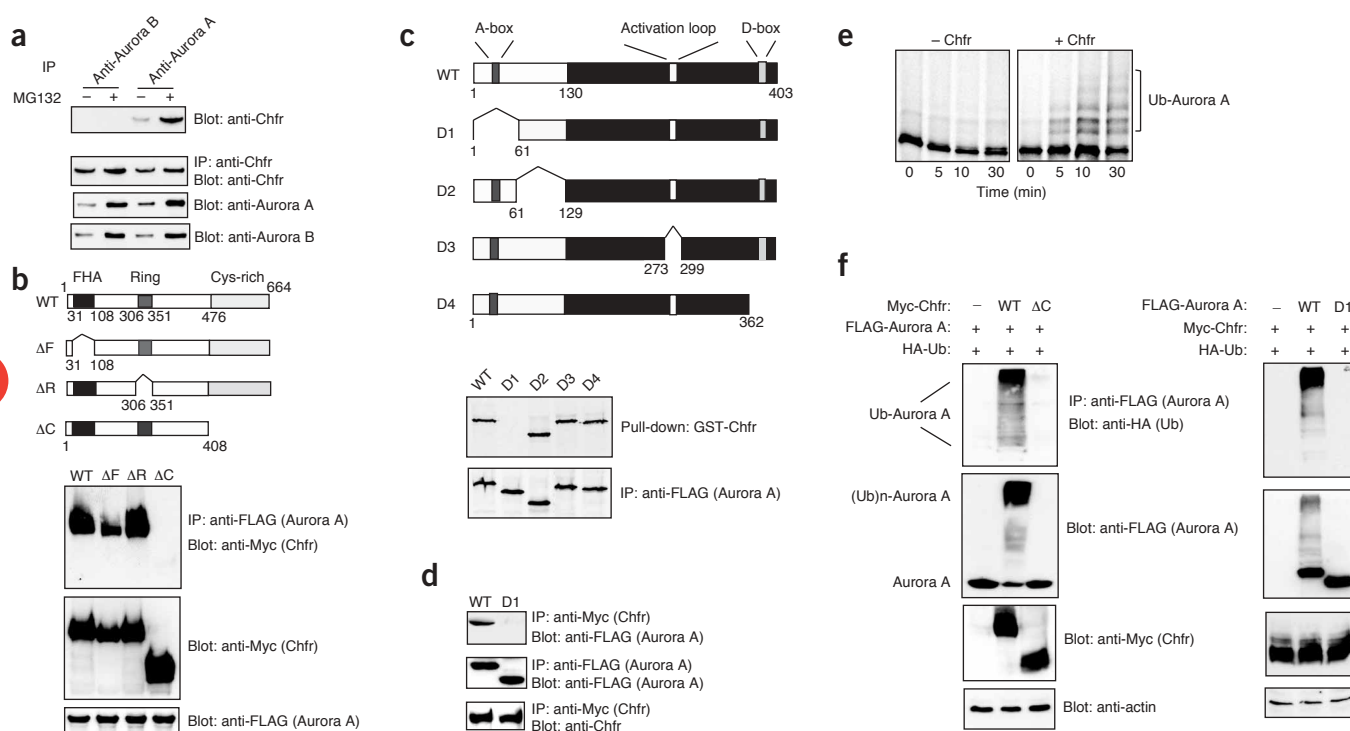


Figure 5 Chfr interacts with Aurora A and ubiquitinates Aurora A both *in vitro* and *in vivo*. (a) Chfr interacts with endogenous Aurora A, but not Aurora B. 293T cells were treated with MG132 (15 μ M) or left untreated. Cell lysates were immunoprecipitated (IP) and immunoblotted with indicated antibodies. (b) The C-terminal cysteine-rich region of Chfr is required for its interaction with Aurora A. 293T cells were cotransfected with plasmids encoding Myc-tagged Chfr and FLAG-tagged Aurora A. Cell lysates were immunoprecipitated (IP) and immunoblotted with indicated antibodies. WT, wild-type; Δ F, FHA domain deletion; Δ R, Ring domain deletion; Δ C, cysteine-rich domain deletion. (c) The N-terminal region of Aurora A mediates its association with Chfr. *In vitro*-translated wild-type or deletion mutants (D1–D4) of Aurora A were pulled-down by GST-Chfr and examined by autoradiography. IP, immunoprecipitation. (d) 293T cells were transfected with plasmids encoding Myc-tagged Chfr and FLAG-tagged wild-type or D1 mutant Aurora A. Cell lysates were immunoprecipitated (IP) and immunoblotted with indicated antibodies. (e) *In vitro*-translated Aurora A was ubiquitinated (Ub) in the presence or absence of recombinant GST-Chfr. The ubiquitination of Aurora A was analyzed by SDS-PAGE. (f) Chfr ubiquitinates (Ub) Aurora A *in vivo*. HCT116 cells were transfected with plasmids encoding FLAG-tagged wild-type or D1 mutant Aurora A, hemagglutinin-tagged ubiquitin (HA-Ub) and Myc-tagged wild-type or Δ C mutant Chfr. Cells were treated with MG132 (15 μ M) for 3 h and then collected for analyses.

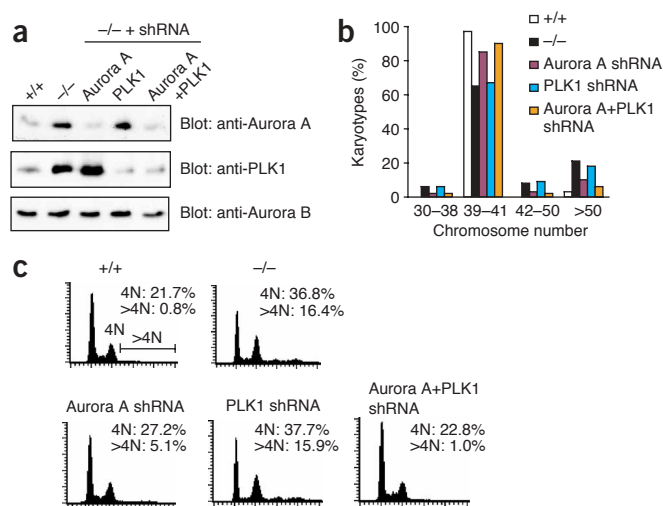


Figure 6 Downregulation of Aurora A decreases the aneuploidy observed in *Chfr*^{-/-} MEFs. P1 MEFs were treated with Aurora A or PLK1 shRNA until P4. (a) Cell lysates were immunoblotted with indicated antibodies. (b) Chromosome numbers of 100 metaphase spreads per sample. (c) Cell cycle distributions of these samples.

Because *Chfr* is involved in mitotic checkpoint control, we next examined whether chromosomal stability was compromised in *Chfr*-deficient cells. We prepared wild-type and *Chfr*-deficient mouse embryonic fibroblasts (MEFs) from embryos at embryonic day 13.5 for *in vitro* culture. After four passages (P4), we prepared metaphase spreads of *Chfr*^{+/+} and *Chfr*^{-/-} cells and determined chromosome numbers. More than 30% of metaphase *Chfr*^{-/-} MEFs showed substantial aneuploidy or polyploidy, whereas *Chfr*^{+/+} MEFs had normal or nearly normal karyotypes (Fig. 3a,b). In addition, *Chfr*^{-/-} MEFs formed spontaneous colonies in *in vitro* culture (Supplementary Fig. 2 online), suggesting that *Chfr*^{-/-} cells have transformation potential. Flow cytometry analysis confirmed that nearly 17% of *Chfr*^{-/-} MEFs contained more than 4N genomic DNA (Fig. 3c). Compared with wild-type MEFs, *Chfr*^{-/-} MEFs had a smaller S-phase population and a greater 4N population. To examine whether the 4N cells were in G2-M phase or were the polyploid cells, we carried out immunofluorescence microscopy using a mitotic marker, phosphorylated histone H3. We did not observe any substantial increase in G2 (indicated by punctuated staining with antibody to histone H3 phosphorylated at Ser10) or M phase cells (indicated by staining with DAPI and antibody to histone H3 phosphorylated at Ser10) in *Chfr*^{-/-} MEFs. Instead, we found many multinucleated cells in *Chfr*^{-/-} MEFs, which may represent the increased populations of 4N and >4N cells (Fig. 3d). To examine mitosis in *Chfr*^{-/-} MEFs, we followed individual mitotic cells using time-lapse microscopy. We observed prolonged prophase and anaphase in *Chfr*^{-/-} MEFs (Fig. 3e). We also observed several types of mitotic errors, including lagging chromosomes, failed nuclear segregation and cytokinesis failure (Fig. 3f), suggesting that *Chfr* is required for proper mitotic transitions.

We observed increased tumor incidence, aneuploidy and defective chromosomal segregation and cytokinesis in *Chfr*-deficient mice and cells. These phenotypes are very similar to those observed in cells with overexpression of Aurora A, a putative oncoprotein involved in mitosis²⁶. Amplification and overexpression of Aurora A have been observed in many primary tumors including breast, colorectal and

gastric cancer^{3,4,27,28}. Like *Chfr*, overexpression of Aurora A in wild-type MEFs induces chromosome segregation defects and cytokinesis failure, which results in aneuploidy and polyploidy^{29,30}. The marked similarities between *Chfr* deficiency and Aurora A overexpression prompted us to explore a potential mechanistic link between these two proteins.

Because *Chfr* is an E3 ubiquitin ligase that may be involved in regulating protein degradation, we first examined the expression levels of Aurora A in wild-type and *Chfr*-deficient cells. The expression levels of Aurora A inversely correlated with those of *Chfr* in MEFs (Fig. 4a), suggesting that *Chfr* may negatively regulate the expression of Aurora A. PLK1, a known substrate of *Chfr*¹⁶, was also upregulated in *Chfr*^{-/-} cells. As a control, we showed that the level of another mitotic kinase, Aurora B, was unchanged in *Chfr*^{-/-} MEFs. *In vitro* culture led to increased 4N and >4N populations in *Chfr*^{-/-} MEFs (Fig. 3c). To exclude the possibility that the increased Aurora A expression is due to the change in cell cycle profile, we determined the levels of Aurora A in first-passage (P1) wild-type and *Chfr*^{-/-} MEFs, which have comparable cell cycle distributions. We still observed increased Aurora A levels in *Chfr*^{-/-} MEFs (Fig. 4b). We also observed increased Aurora A expression in tissues from *Chfr*^{-/-} mice (Fig. 4c).

As an E3 ubiquitin ligase, *Chfr* may directly target Aurora A for ubiquitination and degradation. Because many E3 ligases interact with their substrates, we examined whether *Chfr* bound to Aurora A. Endogenous *Chfr* coimmunoprecipitated with Aurora A but not with Aurora B (Fig. 5a). Aurora A expression and association with *Chfr* also increased after treatment with the proteasome inhibitor MG132. We further determined that the C-terminal cysteine-rich domain of *Chfr* mediates this interaction with the N terminus of Aurora A (Fig. 5b-d). Next, we examined whether Aurora A was a substrate of *Chfr*. *Chfr* promoted polyubiquitination of Aurora A *in vitro* (Fig. 5e). To test whether *Chfr* could ubiquitinate Aurora A *in vivo*, we cotransfected HCT116 cells with plasmids encoding ubiquitin, Aurora A and *Chfr*. Aurora A (Fig. 5f), but not Aurora B (Supplementary Fig. 3 online), was ubiquitinated only when it was cotransfected with wild-type *Chfr*, suggesting that *Chfr* could promote Aurora A ubiquitination *in vivo* (Supplementary Fig. 4 online). Neither the *Chfr* deletion mutant missing the C-terminal cysteine-rich domain nor the Aurora A N terminus deletion mutant could promote the *Chfr*-dependent ubiquitination of Aurora A (Fig. 5f), suggesting that a specific interaction between *Chfr* and Aurora A is required for the *Chfr*-dependent ubiquitination of Aurora A *in vivo*. Taken together, these data suggest that Aurora A is a physiological substrate of *Chfr* *in vivo*.

To explore whether overexpression of Aurora A accounts for the increased aneuploidy observed in *Chfr*^{-/-} cells, we used short hairpin RNA (shRNA) to downregulate expression of Aurora A (Fig. 6a). Decreasing expression of Aurora A, but not that of PLK1, reduced aneuploidy and the number of multinucleated cells in *Chfr*^{-/-} MEFs (Fig. 6b,c), suggesting that Aurora A is the key component downstream of *Chfr* in mitotic control. Notably, downregulation of both Aurora A and PLK1 was more effective in preventing chromosomal instability in *Chfr*^{-/-} MEFs (Fig. 6b,c), implying that Aurora A and PLK1 may work together to ensure normal mitotic progression.

In summary, we show that *Chfr* is a tumor suppressor. *Chfr* functions by regulating the expression level of Aurora A and maintaining genomic stability. Our results imply that disruption of the *Chfr*-Aurora A pathway promotes tumorigenesis and support the hypothesis that chromosomal instability could contribute to tumorigenesis in humans.

METHODS

Generation of knockout mice. We designed the *Chfr* gene-targeting vector to replace an exon spanning nt 132–237 of the mouse gene *Chfr* with the PGK-neo cassette. We cloned genomic DNA fragments flanking this exon into the pKO Scrambler NTKV-1901 vector (Stratagene). We electroporated 129/SvE ES cells with the targeting vector and screened ~300 G418-resistant ES clones by Southern-blot analysis using a probe that hybridizes to a 5.7-kb *Hind*III restriction fragment in wild-type cells and a 7.4-kb fragment in homologous recombinants. We injected two independent ES clones with homologous integration at the targeting site into C57BL/6 blastocysts to generate chimeric mice. We then crossed these chimeras with C57BL/6 females and used heterozygous mice with successful germline transmission of the targeted allele to generate *Chfr*^{-/-} mice. We used PCR to distinguish mouse genotypes using a common antisense primer outside of the target exon, a sense primer in the target exon and a sense primer in the *neo* gene (primer sequences available on request).

Plasmids and antibodies. cDNA encoding FLAG–Aurora A inserted into pSG5 was a gift from D.-S. Lim (Korea Advanced Institute of Science and Technology). We inserted an expressed-sequence tag clone containing the full-length *Chfr* open reading frame into the pA3M vector to generate a mammalian expression construct for three Myc-epitope tagged *Chfr*. We obtained the hemagglutinin-ubiquitin construct from D. Haines (Temple University) and the wild-type and mutant His-ubiquitin constructs from R. Baer (Columbia University). We purchased rabbit antibody to human Aurora A from Cell Signaling Technology. We raised rabbit antibody to mouse Aurora A against Aurora A N terminus peptide (SRPVKTTVPFGPKRVLVTEQIPC) or C terminus peptide (CTGHTSKEPTSKSS). We purchased rabbit antibody to PLK1 from Upstate. We raised rabbit antibody to Aurora B against Aurora B peptides (MAQKENSYPWYGRQTAC and AHPWVRANSRRVLPSSAKKC) and rabbit antibody to *Chfr* against the Ring domain of *Chfr* (residues 259–488). We purchased mouse antibody to FLAG (M2) from Sigma and mouse antibody to His6 conjugated with peroxidase from Roche.

Generation of *Chfr* and Aurora A mutants, cell transfection, immunoprecipitation and immunoblotting. We generated all *Chfr* and Aurora A mutants using the Quickchange site-directed mutagenesis kit (Stratagene). We carried out cell transfection, preparation of cell lysates, immunoprecipitation and immunoblotting in accordance with standard protocols. For coimmunoprecipitation, we treated cells with MG132 (15 μ M) for 10 h before cell lysis. For the *in vivo* ubiquitination assay, we treated transfected cells with MG132 (15 μ M) for 3 h and used biotin-conjugated antibody to hemagglutinin to detect ubiquitinated Aurora A. For demethylation of the *Chfr* promoter in HCT116 cells, we incubated cells with 5 μ M 5-aza-2'-deoxycytidine for 80 h before cell lysis.

Treatment of newborn mice with DMBA. We applied 50 μ l of 0.5% DMBA (Sigma) in acetone to the dorsal skin on postnatal day 3 and killed mice 4 months later. Skin polyps (>5 mm) were counted, excised and assessed by staining with hematoxylin and eosin.

Generation and culture of MEFs, karyotype analysis, flow cytometry analysis, immunofluorescence staining and time-lapse microscopic analysis. We isolated MEFs from embryos at embryonic day 13.5 and maintained them in Dulbecco's modified Eagle medium with 10% fetal bovine serum. To prepare metaphase spreads, we treated MEFs (at P4) with 50 ng ml⁻¹ colcemid (GIBCO BRL) for 6 h at 37 °C. We collected cells, washed them with phosphate-buffered saline and suspended them in 75 mM KCl at room temperature for 15 min. We fixed cells in Carnoy's solution (75% methanol, 25% acetic acid), and dropped 15- μ l aliquots onto slides and stained them with 5% Giemsa solution. We observed metaphase spreads under light microscopy and determined chromosome numbers. For fluorescence-activated cell-sorting analysis, we collected MEFs and stained them with propidium iodide. We determined cell cycle profiles using Cell-Quest. To detect multinucleated cells, we fixed MEFs with 3% paraformaldehyde and stained them with fluorescein isothiocyanate-conjugated rabbit antibody to α -tubulin (SIGMA) and DAPI. For time-lapse microscopic analysis, we infected MEFs with retrovirus encoding histone H2B-EGFP twice. We examined mitotic cells every 2.5 min.

shRNA infection. Lentiviral shRNA expression vector pLL3.7 was a gift from L. Van Parijs (Massachusetts Institute of Technology). The targeting sequences of Aurora A are GACCACTGTTCCCTTCGGT, GCAGGCATCCTTGAGAAG and GTTTGGAAATGTCTACTTG; the targeting sequence of PLK1 is GAAAT TCTGGAGGCTCTAG. We inserted shRNA sequences into pLL3.7 between *Hpa*I and *Xho*I. We carried out lentivirus packaging and infection in accordance with instructions from Invitrogen (Lentiviral support kit K4970-00). Because pLL3.7 also encodes EGFP, positively infected cells can be observed under fluorescence microscopy. Infection efficiency is normally more than 80–90%.

Preparation of tissue lysates. We collected liver (100 mg) and spleen (100 mg) from 12-week-old wild-type and *Chfr*^{-/-} mice. We minced tissues between two microscope slides. We collected cells and lysed them with NETN buffer (0.5% Nonidet-P40, 2 mM EDTA, 50 mM Tris-HCl (pH 8.0) and 100 mM NaCl).

In vitro translation and in vitro ubiquitination assay. Full-length Aurora A was transcribed and translated using the TNT quick coupled transcription/translation system (Promega). We carried out the *in vitro* ubiquitination assay as previously described¹⁶.

Note: Supplementary information is available on the Nature Genetics website.

ACKNOWLEDGMENTS

We thank D. Lim, D. Haines, E. Nigg, S. Sen, T. Takahashi, J. Cheng, R. Baer, L. Van Parijs, J. Chien and K. Minn for reagents and help; J. Woods for proofreading the manuscript; and S. Kaufmann and W. Earnshaw for suggestions. This work is supported in part by the Mayo Clinic Cancer Center and the Breast Cancer Research Foundation. J.C. is a recipient of the Department of Defense breast cancer career development award.

COMPETING INTERESTS STATEMENT

The authors declare that they have no competing financial interests.

Received 9 November 2004; accepted 16 February 2005

Published online at <http://www.nature.com/naturegenetics/>

1. Carmena, M. & Earnshaw, W.C. The cellular geography of aurora kinases. *Nat. Rev. Mol. Cell. Biol.* **4**, 842–854 (2003).
2. Katayama, H., Brinkley, W.R. & Sen, S. The Aurora kinases: role in cell transformation and tumorigenesis. *Cancer Metastasis Rev.* **22**, 451–464 (2003).
3. Bischoff, J.R. *et al.* A homologue of *Drosophila* aurora kinase is oncogenic and amplified in human colorectal cancers. *EMBO J.* **17**, 3052–3065 (1998).
4. Zhou, H. *et al.* Tumour amplified kinase STK15/BTAK induces centrosome amplification, aneuploidy and transformation. *Nat. Genet.* **20**, 189–193 (1998).
5. Littlepage, L.E. *et al.* Identification of phosphorylated residues that affect the activity of the mitotic kinase Aurora A. *Proc. Natl. Acad. Sci. USA* **99**, 15440–15445 (2002).
6. Cleveland, D.W., Mao, Y. & Sullivan, K.F. Centromeres and kinetochores: from epigenetics to mitotic checkpoint signaling. *Cell* **112**, 407–421 (2003).
7. Chan, G.K. & Yen, T.J. The mitotic checkpoint: a signaling pathway that allows a single unattached kinetochore to inhibit mitotic exit. *Prog. Cell Cycle Res.* **5**, 431–439 (2003).
8. Lew, D.J. & Burke, D.J. The spindle assembly and spindle position checkpoints. *Annu. Rev. Genet.* **37**, 251–282 (2003).
9. Cahill, D.P. *et al.* Mutations of mitotic checkpoint genes in human cancers. *Nature* **392**, 300–303 (1998).
10. Imai, Y., Shiratori, Y., Kato, N., Inoue, T. & Omata, M. Mutational inactivation of mitotic checkpoint genes, hMAD2 and hBUB1, is rare in sporadic digestive tract cancers. *Jpn. J. Cancer Res.* **90**, 837–840 (1999).
11. Scolnick, D.M. & Halazonetis, T.D. *Chfr* defines a mitotic stress checkpoint that delays entry into metaphase. *Nature* **406**, 430–435 (2000).
12. Matsusaka, T. & Pines, J. *Chfr* acts with the p38 stress kinases to block entry to mitosis in mammalian cells. *J. Cell Biol.* **166**, 507–516 (2004).
13. Stavridi, E.S. *et al.* Crystal structure of the FHA domain of the *Chfr* mitotic checkpoint protein and its complex with tungstate. *Structure (Camb)* **10**, 891–899 (2002).
14. Murone, M. & Simanis, V. The fission yeast *dma1* gene is a component of the spindle assembly checkpoint, required to prevent septum formation and premature exit from mitosis if spindle function is compromised. *EMBO J.* **15**, 6605–6616 (1996).
15. Guertin, D.A., Venkatram, S., Gould, K.L. & McCollum, D. *Dma1* prevents mitotic exit and cytokinesis by inhibiting the septation initiation network (SIN). *Dev. Cell* **3**, 779–790 (2002).
16. Kang, D., Chen, J., Wong, J. & Fang, G. The checkpoint protein *Chfr* is a ligase that ubiquitinates PLK1 and inhibits Cdc2 at the G2 to M transition. *J. Cell Biol.* **156**, 249–259 (2002).
17. Chaturvedi, P. *et al.* *Chfr* regulates a mitotic stress pathway through its RING-finger domain with ubiquitin ligase activity. *Cancer Res.* **62**, 1797–1801 (2002).

18. Bothos, J., Summers, M.K., Venere, M., Scolnick, D.M. & Halazonetis, T.D. The Chfr mitotic checkpoint protein functions with Ubc13-Mms2 to form Lys63-linked polyubiquitin chains. *Oncogene* **22**, 7101–7107 (2003).
19. Erson, A.E. & Petty, E.M. CHFR-associated early G2/M checkpoint defects in breast cancer cells. *Mol. Carcinog.* **39**, 26–33 (2004).
20. Mizuno, K. *et al.* Aberrant hypermethylation of the CHFR prophase checkpoint gene in human lung cancers. *Oncogene* **21**, 2328–2333 (2002).
21. Shibata, Y. *et al.* Chfr expression is downregulated by CpG island hypermethylation in esophageal cancer. *Carcinogenesis* **23**, 1695–1699 (2002).
22. Corn, P.G. *et al.* Frequent hypermethylation of the 5' CpG island of the mitotic stress checkpoint gene Chfr in colorectal and non-small cell lung cancer. *Carcinogenesis* **24**, 47–51 (2003).
23. Toyota, M. *et al.* Epigenetic inactivation of CHFR in human tumors. *Proc. Natl. Acad. Sci. USA* **100**, 7818–7823 (2003).
24. Mariatos, G. *et al.* Inactivating mutations targeting the chfr mitotic checkpoint gene in human lung cancer. *Cancer Res.* **63**, 7185–7189 (2003).
25. Satoh, A. *et al.* Epigenetic inactivation of CHFR and sensitivity to microtubule inhibitors in gastric cancer. *Cancer Res.* **63**, 8606–8613 (2003).
26. Ewart-Toland, A. *et al.* Identification of Stk6/STK15 as a candidate low-penetrance tumor-susceptibility gene in mouse and human. *Nat. Genet.* **34**, 403–412 (2003).
27. Sen, S., Zhou, H. & White, R.A. A putative serine/threonine kinase encoding gene BTAK on chromosome 20q13 is amplified and overexpressed in human breast cancer cell lines. *Oncogene* **14**, 2195–2200 (1997).
28. Tanner, M.M. *et al.* Frequent amplification of chromosomal region 20q12-q13 in ovarian cancer. *Clin. Cancer Res.* **6**, 1833–1839 (2000).
29. Meraldi, P., Honda, R. & Nigg, E.A. Aurora A overexpression reveals tetraploidization as a major route to centrosome amplification in p53^{-/-} cells. *EMBO J.* **21**, 483–492 (2002).
30. Anand, S., Penrhyn-Lowe, S. & Venkitaraman, A.R. AURORA A amplification overrides the mitotic spindle assembly checkpoint, inducing resistance to Taxol. *Cancer Cell* **3**, 51–62 (2003).